FAILURE MODE SHIFTS IN FATIGUE OF SANDWICH BEAMS

Dan Zenkert and Magnus Burman
Dept. Aeronautical and Vehicle Engineering
Kungliga Tekniska Högskolan, SE-10044 Stockholm, Sweden
danz@kth.se, mburman@kth.se

SUMMARY

Sandwich beams are designed and tested in fatigue, and it is found that for high load and small number of cycles to failure, the beams fail by face tensile fracture. For lower loads, and large number of cycles to failure, the beams fail by core shear.

Keywords: Sandwich, fatigue, beams, failure modes

INTRODUCTION

Sandwich structures offer many potential advantages such as high relative stiffness and strength to weight ratios which is utilised in many weight critical applications. A challenge in the design of sandwich structures is to accurately predict the many potential modes of failure that may occur. Two of the most obvious competing failure modes in the design of simple sandwich beams and panels are face tension/compression fracture and core shear failure. For static loading conditions, one can actually choose which failure mode should be active by appropriate design of the beam or panel, simply by ensuring that the load required for one failure mode is sufficiently higher than for another. In shipbuilding for example, this is commonly utilised. Underwater panels in composite sandwich ships are normally designed so that core shear failure appears before fracture of the laminates. In this way, the panel can fracture, but still be watertight. In fatigue loading, the design towards particular failure modes is slightly more complex, and this is what this paper deals with.

Some early work on fatigue of foam core sandwich structures were performed by Burman *et al* [1-2], Shenoi *et al* [3]], Kanny *et al* [4-5] and Kulkarni *et al* [6]. They all used beam bending tests, designed for core shear failure, to find the fatigue response of foam cores subjected to shear loading. The testing resulted in stress-life relations for various polymeric foam cores. In [7] the authors used an initial flaw approach model through which the crack propagation data could be transformed to stress-life curves. The model gave excellent agreement with measured crack propagation data and tension-tension fatigue testing results for two closed cell polymer foams, the same two foams used herein. In a subsequent investigation, the fatigue behaviour of Rohacell WF-foams in tension, compression and shear was investigated [8]. It was found that the slope of the stress-life curve was different for different load cases and relative densities.

Since sandwich structures also can fail by face sheet failure, the fatigue behaviour of the face sheet laminates also needs to be established. There exists quite a lot of information about fatigue of composite laminates in the literature, albeit more limited concerning

laminates made from NCF-fabrics. Kahn and Mouritz [9] compared stitched and non-stiched composite laminates and concluded that the stitching has a negative influence on the tensile fatigue performance. The same conclusions were drawn from a later investigation [10]. Gagel *et al* [11,12] studied the formation of cracks and stiffness degradation of glass-fibre NCF-laminates subjected to tensile fatigue loading concluding that some of the micro-crack formation processes are the same as under quasi-static loading. They also developed a model for the mechanical degradation under fatigue loading. Vallons *et al* [13,14] studied the formation of micro-cracks in carbon fibre NCF-laminated under fatigue loading. They used Acustic Emission (AE) techniques and X-ray imaging to study micro-cracks and experimental measured the stiffness degradation. An interesting finding was that for a $[+45/-45]_s$-laminate the fatigue endurance limit (the strain under which there is an apparent infinite fatigue life) can be found from the linear part of the stress-strain relation in a simple tensile test. For $[0/90]_s$ it seems that the fatigue endurance limit is well above the stress level for damage initiation under static loads. Aono *et al* [15] performed tension-tension and tension-compression fatigue experiments on [+45/-45] NCF-laminates. There are two interesting observations from this work; testing at R = -1 gives higher fatigue life than at R = 0.1, and the failure modes are different. In a subsequent paper, Aono *et al* [16] also studied glass fibre NCF-laminates and used replica methods to monitor fatigue damage progression under tensile fatigue loading. They found that damage was first initiated near the stitches, in resin rich regions.

An industrial sector where fatigue of composite laminates is very important is in wind power. Many wind turbine blades are made from glass NCF's and fatigue is one of the main design constraints [17]. There is a very comprehensive investigation of fatigue of laminates for wind turbine applications made by Nijssen [18]. There are some constant amplitude data in there, though most of the work focuses on spectrum fatigue loading.

This paper will not deal with a detailed description of the fatigue damage progression but will study fatigue as a design problem. It is rationalised that even if a sandwich structure is designed to fail with a given failure mode (e.g. core shear failure) under quasi-static loads, the failure mode can shift (to e.g. face sheet failure) under fatigue loading. The foundation for this rationale is that the slope of the stress-life relations for different failure modes can be different. Thus, the same structure, with the same material combination, under the same loading condition but with different loading amplitude, a sandwich structure can have different failure modes in fatigue.

MATERIALS

Two high performance, rigid polymer foams with closed cell structure were used in this study; Divinycell H-grade and Rohacell WF-grade. Divinycell is a cross-linked rigid cellular PVC foam and it is produced in a variety of densities where mechanical properties (higher strength and moduli) increase with density. The quality used here was H100, with a nominal density of 100 kg/m^3. Any details on this material can be found in [19]. The other core material used in this study is Rohacell, a PMI foam with predominantly closed cells but is more brittle than the PVC foam. The quality used herein was WF51, where WF is the particular grade of Rohacell and the number corresponds to the nominal density in kg/m^3. Details on this material can be found in [20]. The reason for choosing these two materials is that one exhibits a fairly brittle behaviour (Rohacell) in the context of foams and the other (Divinycell) has a more

ductile behaviour (higher strain to failure, a more pronounced plastic regime). They further exhibit different behaviour in fatigue. Both materials are close to being isotropic, with only small variations in moduli and strengths in the in-plane and out-of-plane directions.

The laminates used herein were made from glass-fibre NCF fabrics of the type DBLT-850-E10 [21]. This is a quadriaxial non-crimp fabric (NCF) with approximately equal amount of fibres, approximately 200 g/m^2, in four main directions in the sequence [0/45/90/-45]. The laminates were manufactured using a vacuum infusion process (VARTM) with Reichhold DION 9500 Vinylester. A single layer of DBLT-850 builds approximately 0.75 mm after infusion. Typical material data for the cores and the laminates are given in Table 1. The yield stress for the cores are defined as the 1% offset stress.

Table 1 Basic material data for the material used.

	WF51	H100	Laminate
E [MPa]	75	126	15,000
G [MPa]	27	40	-
σ_1 [MPa]	1.6	3.3	310
τ_{yield} [MPa]	0.66	1.13	-
$\tau_{failure}$ [MPa]	0.77	1.21	

SHEAR FATIGUE TESTING OF CORE MATERIALS

A four point bending rig which enables fatigue loading with both positive and negative loads was used in this investigation, as depicted schematically in Fig.1a. This design allows the supports to rotate around the neutral axis of the beam in order to minimise the stress concentrations near the load introductions. Furthermore the supports are movable in the beam length direction to enable varying settings of L_1 and L_2 (see Fig.1a). The supports are also covered with rubber pads in order to smooth out the load transfer. The outer load arms are allowed to move horizontally thus preventing any membrane forces to occur.

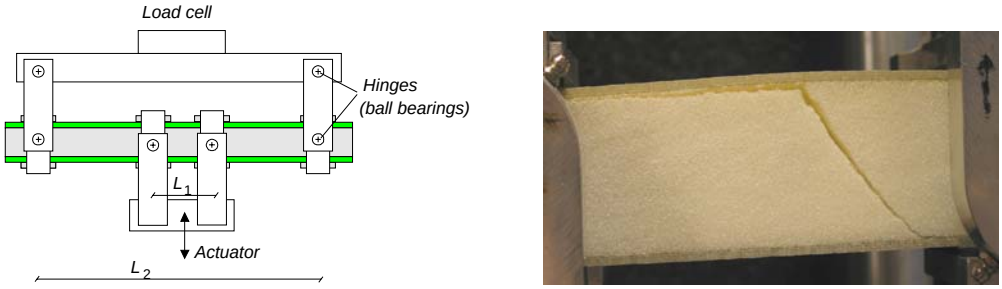

(a) (b)

Figure 1 (a) Schematic set-up for fatigue testing of foams using four-point bending test. (b) Photograph of a fractured WF51 test specimen in the test rig.

All specimens were 500 mm long, a width equal to the thickness, and tested using the set-up, L_1 = 80 mm and L_2 = 440 mm. A 50 mm thick core was used with approximately 4 mm thick faces. The testing was performed at R = 0.1 at a testing frequency of 2 Hz.

The shear failure in fatigue of the WF51 specimens is similar to that under quasi-static loading with a sudden shear crack appearing, Fig.1b. For the H100-specimens, the core appears to collapse in a horizontal band, but the beam does not really suddenly fracture.

The results from this testing is shown in Fig.2a as standard stress-life relations plotted in double logarithmic scale. The dashed lines in Fig.2 represent the yield stress in shear for the foam. This is defined by the 0.2% offset stress [8]. There are a few things to notice in Fig.2. Above the yield stress, the fatigue life has very large scatter, which is clearly seen for the H100 material. Therefore, high-cycle fatigue is defined for stress levels below the yield point. The number of cycles to failure at yield is different for the two materials; approximately 10^2 for WF51 and 10^4 for H100. Another important thing is that the slope of the fatigue life relation in the high-cycle fatigue regime is different. The stress-life data can be adapted to a Basquin's law type relation that reads

$$\Delta\sigma = B(N)^{-1/\beta} \tag{1}$$

where $\Delta\sigma$ is the stress range, N the number of cycles to failure, B a fitting constant and $-1/\beta$ the slope of the relation. The fitted data in Fig.2 gives the slope β to approximately 20 for WF51 and 12 for H100.

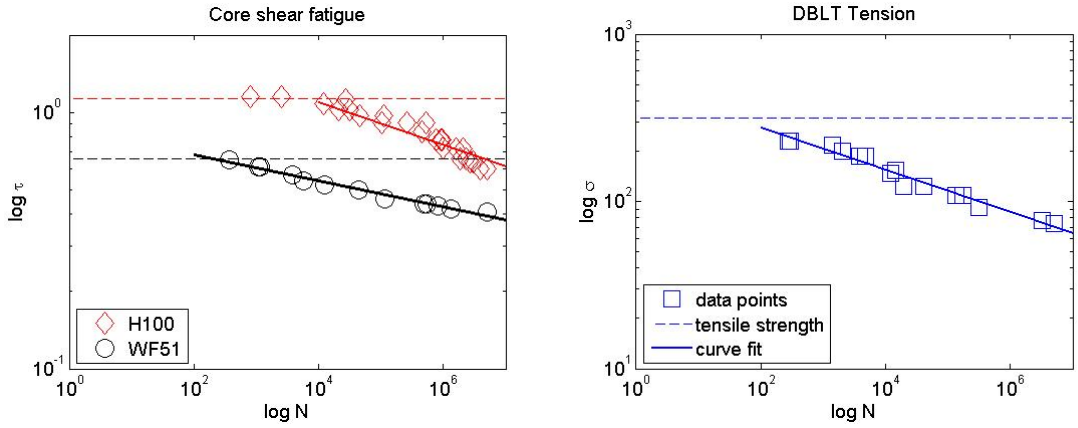

(a) (b)

Figure 2 (a) Shear fatigue data for H100 and WF51 core, and (b) tensile fatigue data for the DBLT laminate in tension

TENSILE FATIGUE TESTING OF LAMINATES

The tensile fatigue testing of the laminates were performed on laminates consisting of 2 layers of DBLT-850, giving a lay-up sequence of $[0/45/90/-45]_s$ with a total thickness of approximately 1.5 mm. Rectangular, tabbed specimens were used, as shown in Fig.3(a-b). The width of the specimens was 25 mm and the gauge length was 100 mm. The fatigue testing was performed in a standard servo-hydraulic testing machine at 2 Hz and with a loading ratio $R = 0.1$.

The specimens failed abruptly with no or very little visual signs of damage prior to complete rupture. A ruptured specimen is shown in Fig.3c.

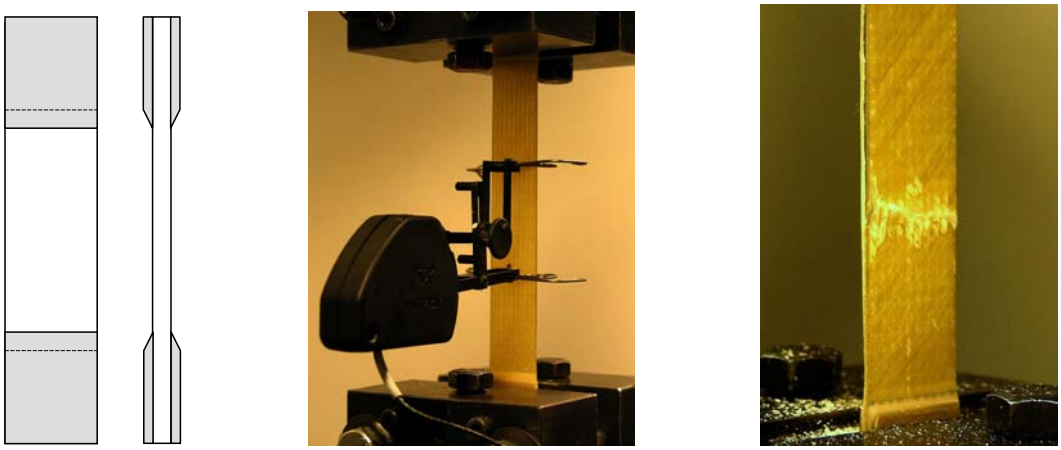

(a) (b) (c)

Figure 3 (a) Schematic set-up for fatigue testing of laminates. (c) Photograph of experimental set-up. (b) Photograph of a fractured laminate in the test rig.

The results of the laminate testing is summarised in Fig.2b by means of a stress-life diagram in double logarithmic scale. The slope, β, according to eq.(1) of this stress-life curve is approximately equal to 8 (7.8). This is similar to what was reported in [17] where a slope of 8.7 can be deduced for tension fatigue at R = 0.1. In the work by Nijssen [18] a slope β = 9.9 is reported. In other investigations, e.g. [14,16] the slope deduced from stress-life relations differs a lot, but appears to be around or above 10 in most cases.

DESIGN OF SANDWICH BEAMS

We now wish to design a sandwich beam that exhibits two competing failure modes; core shear failure and face sheet tensile fracture. Starting from the four-point bending set-up depicted in Fig.4(a), one can formulate the following;

Define the load going into the beam at each support as P = 1 N (unit load). The transverse force between the inner and outer supports, T is then equal to P. Between the inner supports, the transverse force is equal to zero. The bending moment is zero at the outer supports (since they are hinged), linearly increasing towards the inner supports. Between the inner supports, the bending moment is constant and equal to $P(L_2 - L_1)/2$. By using classical sandwich theory, with the assumption of constant core shear stress, one can write the stresses in the core and the face sheets as [22]

$$\sigma_1 = \frac{M}{t_1 d} = \frac{P(L_2 - L_1)}{t_1 d},\ \sigma_2 = \frac{M}{t_2 d} = \frac{P(L_2 - L_1)}{t_2 d} \text{ and } \tau_c = \frac{P}{d} \qquad (2)$$

where t_1 and t_2 are the thicknesses related to the upper and lower face and t_c to the core. The distance between the centreoids of the laminates is $d = (t_1 + t_2 + t_c)/2$, see Fig4(b). If we apply a fatigue load with the ration $R > 0$ so that the lower face sheet is subjected to tension and the upper face sheet to compression, then the tensile stress in the lower face sheet will always be higher than the compressive stress in the upper face sheet if we make a sandwich beam with $t_1 > t_2$. By doing this, we can ensure that face failure will occur in the bottom laminate, subjected to tension. This is a simplification done since we lack data for the fatigue properties of the laminate in compression.

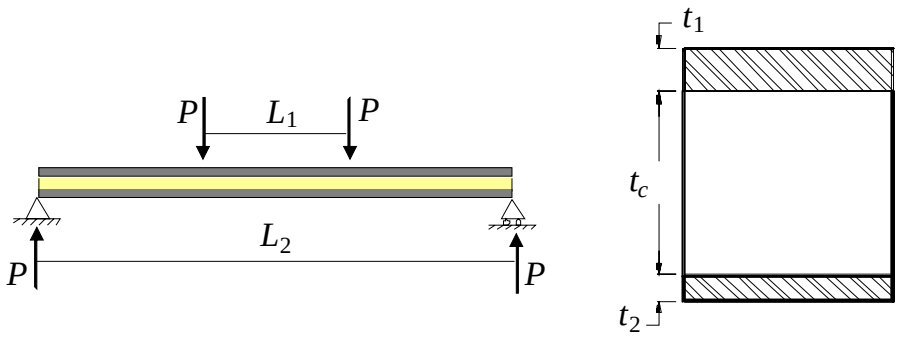

(a) (b)

Figure 4 (a) Schematic of four-point bending set-up and (b) definition of sandwich beam cross-section

By using eqs.(2) one can design a sandwich beam through the use of the parameters t_1, t_2, and t_c, together with the structural geometry, in this case defined simply by L_1 and L_2, towards a specific failure more (face tensile fracture or core shear failure). Take eqs.(2) and rewrite into

$$P = \frac{\sigma_2(N) t_2 d}{L_2 - L_1} \text{ and } P = \tau_c(N) d \tag{3}$$

where the stress is taken as function of fatigue loading cycles to failure according to Fig.2, for the face sheet and core, respectively. In doing so, we get a fatigue life relation for the sandwich beam, i.e. P as function of number of cycles to failure, with two stress-life curves, one for the face sheet and one for the core. These two relations can be altered through appropriate design (choosing t_1, t_2, t_c, L_1 and L_2). The aim now is to design sandwich beams for which the two stress-life relations cross each other for some value of the load, implying that the beam will shift failure mode depending on the amplitude of the fatigue load.

TESTING OF SANDWICH BEAMS

Two sets of sandwich beams were designed in order to attempt to promote failure mode shift in fatigue loading. They are defined in Table 2.

Table 2 Definition of sandwich beam designs used in testing

	Design 1 – H100 core	Design 2 – WF51 core
Upper face sheet	2 layers DBLT- symmetric	2 layers DBLT- symmetric
Lower face sheet	4 layers DBLT- symmetric	4 layers DBLT- symmetric
Core	H100	WF51
t_c [mm]	50	50
t_1 [mm]	3.0	3.0
t_2 [mm]	1.5	1.5
L_1 [mm]	80	175
L_2 [mm]	500	1000

The laminate subjected to tensile stress in the beam tests were in both cases made for a lay-up sequence of $[0/45/90/-45]_s$ and the laminate subjected to compression was twice as thick with a lay-up sequence of $[(0/45/90/-45)_2]_s$. The testing was performed at R = 0.1 at a testing frequency of 2 Hz for the H100 beams, but only 1 Hz for the WF51. The

reason for the lower frequency in that case was simply because the beams were much longer, therefore with more deflection.

The collected results for the H100 and WF51 beams are shown in Fig.5. The dashed horizontal lines represents the load level for assumed quasi-static failure, the upper (blue) line for tensile face sheet fracture and lower (red or black) for core yield. For the H100 beams, Fig.5a, the expected failure load for tensile laminate fracture is 109 N/mm width, and for core failure 59 N/mm width. This beam is thus statically designed for core shear failure. The solid lines represent fatigue data for the materials through the use of eq.(3) and the test results of the cores and laminates. As seen, the design in this case indicates that the failure mode should shift from core shear to face failure when the load is decreased. This happens at a load level when the expected life is slightly less than 10^4 load cycles. The experimental results are almost perfect in this case. Above 10^4 load cycles, the failure mode is tensile face failure and below it is core shear.

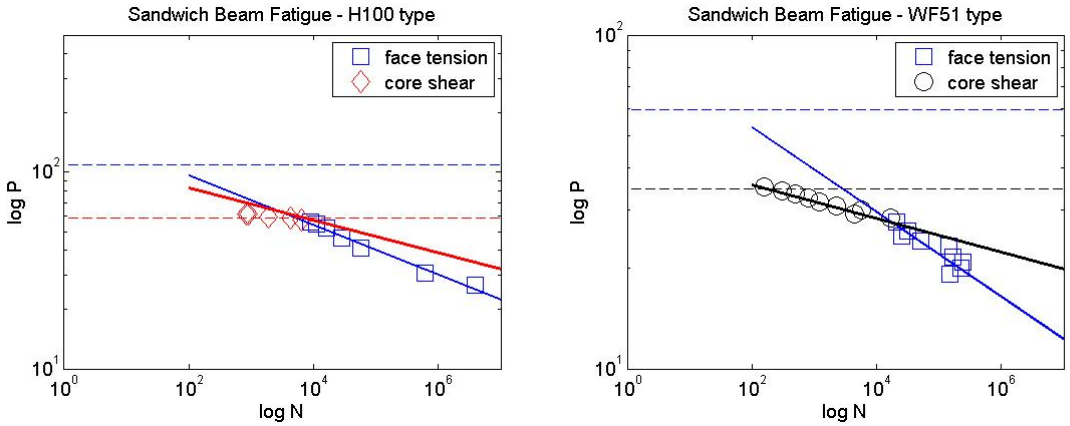

(a) (b)

Figure 5 Test results from four-point bending fatigue testing of (a) H100 beam design and (b) WF51 beam design. Square markers indicate face tensile fatigue failure and diamond and circular markers indicate core shear fatigue failure.

The collected results for the WF51 beams are shown in Fig.5b. The expected failure load for tensile laminate fracture is 60 N/mm width, and for core failure 34.5 N/mm width. As for the H100 beam types, there is a predicted failure mode should shift from core shear to face failure when the load is decreased. This should happen at a load level when the expected life is slightly above 10^4 load cycles. As seen in Fig.5(b) there is again an almost prefect match between the test results and the prediction.

The failure modes are shown in Fig.6. The core shear failure of the H100 beams is a little hard to elude to. The H100 is rather ductile and does not really fail abruptly. Instead, a shear band is created in which the core rather collapses. When this happens the entire beam collapses. To highlight this, horizontal and vertical lines were drawn on the surface of the core. Details on the failure evolution are described in [1]. The face tensile failure appears abruptly without any prior visual signs of degradation.

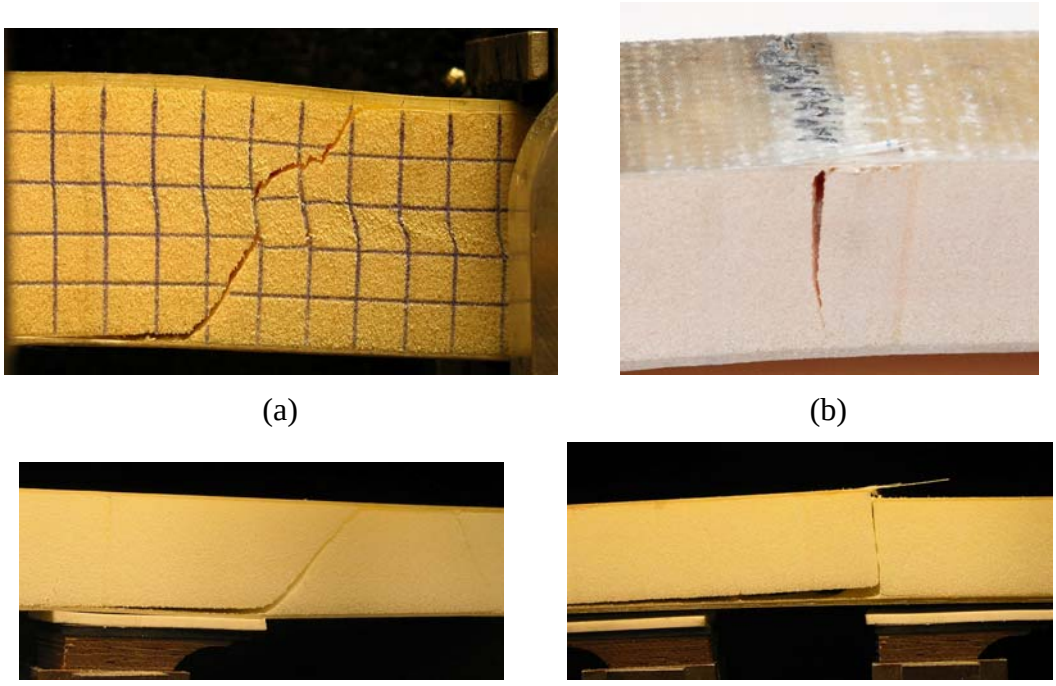

(a) (b)

(c) (d)

Figure 6 Photographs of failure modes. (a) H100 core shear failure, highlighted through painted lines on the core surfaces, (b) H100 beams with tensile face failure, (c) WF51 core shear failure and (d) WF51 beam with laminate failure

The failure modes are shown in Fig.6c and d. The core shear failure is quite obvious in this case. The WF51 is rather brittle and fails abruptly. The face tensile failure also appears abruptly without any prior visual signs of degradation.

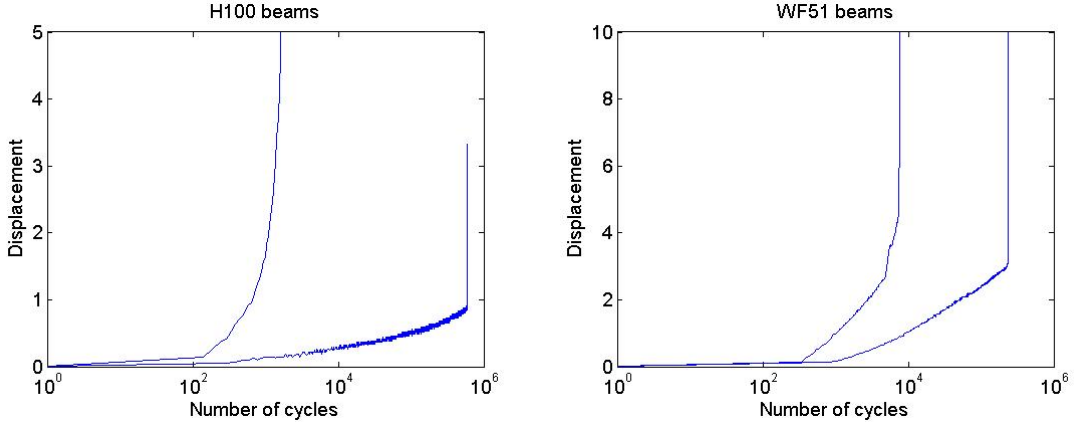

(a) (b)

Figure 7 Testing machine displacement as function of loading cycles for (a) two H100 beams and (b) two WF51 beams showing the creep behaviour.

The H100 beams did exhibit some creep deformation during fatigue testing. The testing machine displacement versus number of cycles are shown in Fig.7a for one beam that failed in shear (few cycles to failure) and one that failed by tensile laminated rupture (large number of cycles to failure). It is seen that there is some creep deformation during cyclic loading. In order to compare correctly one should know that the cyclic

deformation (machine displacement) $\Delta\delta$ was around 13 mm for the beam failing at 1868 cycles and around 6 mm for the beam failing at 6×10^5 cycles. Thus, the increase in relative displacement from the initial load cycles to the point of failure is quite small, being only fraction of millimetres in the case of high load (1868 cycles to failure) and less than 1 mm for the low load case (failure at 6×10^5 cycles).

The WF51 beams did also exhibit some creep during fatigue testing. The testing machine displacement versus number of cycles are shown in Fig.7b for one beam that failed in shear (few cycles to failure) and one that failed by tensile laminated rupture (large number of cycles to failure). It is seen that there is some creep deformation during cyclic loading. In order to compare correctly one should know that the cyclic deformation (machine displacement) $\Delta\delta$ was around 29 mm for the beam failing at 7748 cycles and around 23 mm for the beam failing at 2.37×10^5 cycles. Thus, the increase in relative displacement from the initial load cycles to the point of failure is still small, being only approximately 3 millimetres in both cases.

CONCLUSIONS

Two types of sandwich beams were designed with respect to fatigue performance of the face sheets and the core. The beams were designed with the aim to promote failure mode shifts as the fatigue loading amplitude was changed. The designed beams were manufactured and tested in fatigue. For high loading amplitudes and few cycles to failure, the beams failed by core shear failure. When the load amplitude was decreased the failure mode shifted to face sheet tensile failure. This shows that although a sandwich structure may be designed for core shear failure, at least to quasi-static loading, the failure mode can still be face sheet failure if fatigue loading is applied. The reason for this is that the stress-life life curves for core shear failure and face tensile failure have different slopes.

ACKNOWLEDGEMENTS

The financial support for this investigation has been provided by The Office of Naval Research (ONR) through programme officer Dr. Yapa D.S. Rajapakse (Grant No. N00014-07-1-0344). Evonik and DIAB are acknowledged for supplying the materials. Special thanks to Anders Beckman and Bo Magnusson for help with the manufacturing of the test specimens and the fatigue testing.

References

1. Burman M. and Zenkert D., "Fatigue of Foam Core Sandwich Beams, Part I: Undamaged Specimens", *Int J Fatigue*, 19(7), 1997, pp 551-561
2. Burman M. and Zenkert D., "Fatigue of Foam Core Sandwich Beams, Part II: Effect of Initial Damages", *Int J Fatigue*, 19(7), 1997, pp 563-578
3. Shenoi R.A., Clark S.D. and Allen H.G., “Fatigue Behaviour of Polymer Composite Sandwich Beams”, *J Comp Mat*, 29(18), 1995, pp 2423-2445
4. Kanny K., Mahfuz H., Carlsson L.A., Thomas T. and Jeelani S., “Dynamic mechanical analyses and flexural fatigue of PVC foams”, *Comp Struct*, 58(2), 2002, pp 175-183
5. Kanny K. and Mahfuz H., “Flexural fatigue characteristics of sandwich structures at different loading frequencies”, *Comp Struct*, 67, 2005, pp 403-410

6. Kulkarni N., Mahfuz H., Jeelani S. and Carlsson L.A., ”Fatigue crack growth and life prediction of foam core sandwich composites under flexural loading”, *Comp Struct*, 59(4), 2003, pp 499-505

7. Zenkert D., Shipsha A. and Burman M., “Fatigue of Closed Cell Foams”, *J Sandwich Struct & Mater*, 8(6), 2006, pp 517-538

8. Zenkert D. and Burman M., “Tension, Compression and Shear Fatigue of a Closed Foam”, *Comp Sci Tech*, 69, 2008, pp 785-792

9. Shah Kahn M.Z. and Mouritz A.P., “Fatigue behaviour of stitched GRP laminates”, *Comp Sci Tech*, 56, 1996, pp 695-701

10. Mouritz A.P., “Tensile fatigue properties of 3D composites with through-thickness reinforcement”, *Comp Sci Tech*, 68, 2008, pp 2503-2510

11. Gagel A., Lange D. and Schulte K., “On the relation between crack densities, stiffness degradation, and surface temperature distribution of tensile fatigue loaded glass-fibre non-crimp-fabric reinforced epoxy”, *Compos A*, 37, 2006, pp 222-228

12. Gagel A., Fiedler B and Schulte K., “On modelling the mechanical degradation of fatigue loaded glass-fibre non-crimp fabric reinforced epoxy laminates”, *Comp Sci Tech*, 66, 2006, pp 657-664

13. Vallons K, Mengmeng Z., Lomov S. and Verpoest I., “Carbon composites based on multi-axial multi-ply stitched preforms – Part 6. Fatigue behaviour at low loads: Stiffness degradation and damage development”, *Compos Part A*, 38, 2007, pp 1633-1645

14. Vallons K, Lomov S. and Verpoest I., “Fatigue and post-fatigue behaviour of carbon/epoxy non-crimp fabric composites”, *Compos Part A*, 40, 2009, pp 251-259.

15. Aono Y., Noguchi H., Lee S-H., Kuroiwa T. and Takita K., “Fatigue strength of double-bias mat composites composed of stitched unit layers”, *Int J Fatigue*, 28, 2006, pp 1375-1381.

16. Aono Y., Hirota K., Lee S-H., Kuroiwa T. and Takita K., “Fatigue damage of GFRP laminates consisting of stitched unit layers”, *Int J Fatigue*, 30, 2008, pp 1720-1728.

17. Brøndsted P., Lilholt H. and Lystrup A., ”Composite Materials for Wind Power Turbine Blades”, *Annu Rev Mater Res*, 35, 2005, pp 505-538.

18. Nijssen R., *Fatigue Life Prediction and Strength Degradation of Wind Turbine Rotor Blade Composites*, Doctoral Thesis, KC-WMC and Faculty of Aerospace Engineering, Delft University, The Netherlands, 2006, ISBN-10: 90-9021221-3

19. *Divinycell H-grade*, *Technical Manual*, DIAB AB, www.diabgroup.com

20. *Rohacell WF*, Evonik Industries, www.rohacell.com

21. Devold AMT, Quadriaxial reiforcements, www.amt.no

22. Zenkert D., *An Introduction to Sandwich Construction*, EMAS Ltd, Warley, UK, 1995